*Journal of Applied Fluid Mechanics*, Vol. 13, No. 2, pp. 753-766, 2020.
Available online at www.jafmonline.net, ISSN 1735-3572, EISSN 1735-3645.
DOI: 10.29252/jafm.13.02.30356

# Thermodynamics of a Liquid Film in the Presence of External Shear Stress

S. A. Alkharashi[1,2†] and A. Assaf[3]

[1] *Applied Sciences Department, College of Technological Studies, PAAET, Kuwait*
[2] *Quesnafig Technical College, Ministry of Higher Education, Cairo, Egypt*
[3] *Mathematics Department, Faculty of Science, Helwan University, Egypt*

†*Corresponding Author Email: sa.alkharashi@paaet.edu.kw*

(Received April 6, 2019; accepted July 20, 2019)

## ABSTRACT

This study aims to discuss and illustrate the role of insoluble surfactants on the stability analysis of a shear-imposed free surface motion down an oblique heated substrate. The couple effects of temperature and surfactant concentration gradient on the surface tension are assessed, in which the surface tension of the fluid is assumed to vary linearly on surfactant concentration and the temperature. The exact analytical solutions for the Stokes flow and the long-wave approximation are derived, depending on the linear stability theory, and hence the neutral curves are plotted and discussed. Due to the presence of the surfactant, there are two different modes that impact the stability process of a shear-imposed inclined flow. The current study recovers some limiting cases upon the selected data. The system parameters governing the liquid layer and the substrate geometry have a strong effect on the wave forms and so the stability of the free surface. The influences of various parameters such as Marangoni, Biot, elasticity, surfactant Péclet number and Reynolds numbers, besides the angle of inclination are considered. It is found that, the Reynolds and the surfactant Péclet numbers and the angle of inclination have destabilizing effects.

**Keywords:** Free surface stability; Shear-imposed; Insoluble surfactants; Inclined substrate; Long-wave approximation.

## NOMENCLATURE

| | | | |
|---|---|---|---|
| $B_i$ | Biot number | $\mathbf{t}$ | the corresponding unit tangent |
| $c$ | complex frequency | $Tr$ | the matrix transpose |
| $C_a$ | capillary number | $\mathbf{V}$ | fluid velocity vector |
| $C_p$ | specific heat at constant pressure | x,y | coordinates system |
| $D_s$ | surface diffusion coefficient | $\gamma$ | surface tension |
| g | gravity force | | |
| $h$ | surface deflection | $\nabla$ | gradient operator |
| $k$ | wave number | $\rho$ | fluid density |
| $M_a$ | Marangoni number | p | fluid pressure |
| $\mathbf{n}$ | unit outward normal vector to the surface | $\mu$ | dynamic viscosity |
| $N_e$ | elasticity number | $\beta$ | angle of inclination |
| $P_e$ | Peclet number | $\tau_s$ | imposed shear stress |
| $P_r$ | Prandtl number | $\ell$ | unperturbed film thickness |
| $P_{es}$ | surfactant surface Peclet number | $\boldsymbol{\kappa}$ | thermal conductivity |
| $q$ | uniform heat transfer coefficient | $\Gamma$ | surfactant concentration |
| $R_e$ | Reynolds number | $\psi$ | stream function |
| $T$ | absolute temperature | | |

## 1. INTRODUCTION

Moving a thin layer down an inclined substrate or a vertical plane with a free surface is of interest in a broad range of dynamical studies. The stability of a thin layer flows system along an oblique substrate under the gravity force is performed in many various industries due to its dramatic effect on the manufacturing of microelectronics components, active glass screens, cathode ray tubes, magnetic tapes, computer disks, and in the modern accuracy, coating of photographic

emulsions, and to keep paints protected. Furthermore, the transport rate of mass, heat, and momentum have an important influence in adsorption columns, designing distillation evaporators and condensers and so on.

Due to these handy applications, several re-searches on computational as well as theoretical problems have illustrated that laminar flows are sensitive to the capillary number giving the impact of surface tension strength, and the substrate geometry as well as Reynolds number, which characterizes the evolution methods of a viscous Newtonian liquid layer down a sloping substrate or a vertical plane. Extensive reviews of numerical estimations and analytical methods of the free-boundary problem issue, characterizing, steady moving films down an oblique wall have been investigated by a variety of modes in many types of reports. These discussions display that the wavy structure on the free interface of the layer motion is sensitive to different factors like the slope angle, the longitudinal length of the test section as well as flow rate, further the effects of external forces such as magnetic and electric fields.

Yih (1963), studies the stability behavior of liquid flow down a sloping plane. His result reveals that the imposed system was stable to long-wavelength perturbations at when the Reynolds number is small enough. In a study of the stability process of a magnetic film of a viscous liquid down an oblique substrate under the effect of gravity force, Renardy and Sun (1994) illustrated that the magnetic range has a stabilizing influence on both the surface and shear modes and can be applied to delay the instability behavior. In two-dimensions domain, Tomlin *et al*. (2019), analyzed the nonlinear behavior of the liquid interface, that is dominated by a forced Kuramoto-Sivashinsky relation, in which the non-linearity is assumed to be weakly. In this work, the authors considered the rule of a three-dimensional oblique fluid thin layer. Additional interested studies concerned with the stability of free surface motion are in Uma and Usha (2006), Samanta (2008a,b): Mukhopadhyay and Mukhopadhyay (2009).

In all the works cited above, the free surfaces have been considered to be clean i.e., there are no surfactants diffuse at the dividing surface. The problems involving the phenomena of diffusion for insoluble surfactants at the free surface (or the interface between two fluids) have been increasingly attracting the attention of many researchers. For examples, in the limit of disappearing Reynolds number, Luo and Pozrikidis (2007), investigated the three-dimensional motion of the gravity-driven for a fluid thin layer down an oblique substrate with doubly periodic corrugation, where the layer surface may display surface tension (variable or constant) due to insoluble surfactants.

Based on a Stokes approximation Frenkel and Halpern (2002), discussed the stability picture of a two-liquid shear motion with insoluble surfactants on the separator interface, in which long-wave approximation for the growth rates is reported. Pozrikidis (2003), investigated the effect of insoluble surfactants on the gravity-driven flow of a fluid film down an inclined plane with periodic corrugations or indentations. Marangoni convection in the limit of the long-wave asymptotic in a horizontal fluid film with insoluble surfactants (not into the bulk of the liquid) diffused on the free surface (not into the bulk of the liquid) is the subject of the pa-per by Mikishev and Nepomnyashchy (2010). It is shown that the oscillatory long-wave instability is less serious than monotonic one only for slight, elasticity numbers, if the Lewis number is slight.

In the work by Srivastava and Tiwari (2018) in the presence of an insoluble surfactant depending an embedded, regularly spaced heaters, the stability process of a gravity-driven thin liquid layer is discussed. They investigated that insoluble surfactant plays a stabilizing influence on the imposed system, wherein it reduces the height of the capillary ridge. Yang *et al*. (2018) have performed a numerical illustration of a falling liquid film as an insoluble surfactant is located at the surface. The concentration of surfactant is obtained by the ratio between the surface area of the layer and surfactant mass. Their results illustrated that the surfactant has a considerable effect on the dynamics of the considered liquid thin layer. Wei (2004), examined the impact of insoluble surfactants on the linear stability process of a shear-imposed flow down an oblique substrate, in the long-wavelength limit. The surfactants diffuse on the free surface, not on the bulk of the fluid film. He assumed an additional surface shear, which causes instability as a result of the shear-induced Marangoni influence. Two types of stability are specified, and the associated growth rates are investigated. The linear and nonlinear stability of the effect due to air shear on the interfacial instability is studied by Iqbal (2013). The author investigated that the transverse velocities and stream-wise growing when the falling, shear works in favor of inertial force to reduce the flow stabilization, in which the inverse effect holds for the uphill shear.

Finally, in the presence of surfactants and heat transfer as well as the presence of surface shear-imposed contaminated fluid layers, we cited the following two works the first by Ding and Wong (2013), the authors in this paper studied the linear stability analysis of an insoluble surfactants occurs on the surface of a liquid heated film. Their results show that there are two roles found for the sur-face surfactants; one is stabilized the system when it concentrated and the other is unstable behavior as the diffusion of the surfactant increased. The second, Bhat and Samanta (2019) have recently per-formed the linear stability behavior of a heated liquid film flowing down an inclined substrate the free surface of the layer is subjected to shear-imposed stress in which an insoluble surfactant has covered the interface.

In view of these, in the present study, our main goal has been concentrated, on developing a theory for a two-dimensional free surface the motion of a thin layer of viscous liquid down an oblique heated plane. The free surface is subjected

to additional constant shear stress induced by airflow and a sur-face insoluble surfactants are also presented on the air-liquid interface, not in the bulk of the film.

## 2. FORMULATION OF THE PHYSICAL MODEL

Consider a laminar flow of a thin viscous film with a uniform thickness $\ell$ along a heated oblique surface, which is located at constant temperature $T_w$ as shown in Fig.1.

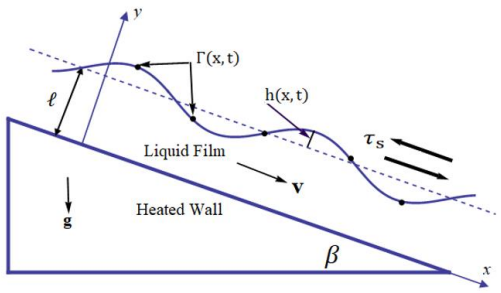


**Fig. 1: Sketch of the profile geometry.**

The coordinate axes are selected such that $x-$ axis along the slope of the plane, in the decline direction, at an angle $\beta \in (0,\pi/2)$ with the horizontal, while $y-$axis orthogonal to the inclined plane. The deflection of the surface prevented by assuming that surface tension and the gravity force are sufficiently large. An additional shear stress $\tau_s$ has a constant value offered by an airflow is made on the free surface and its orientation can either object or support the flow under gravity. Also, insoluble surfactants are diffused on the free surface (not into the bulk of the liquid). If the temperature and surfactant concentration have sufficiently small deviations from their equilibrium quantities $T_a$ and $\Gamma_0$, respectively, we assume that the surface tension linearly varies with the temperature and the surfactants, in which both Marangoni effects are taken into consideration, so that

$$\gamma(\Gamma,T)=\gamma_0(\Gamma_0,T_a)-\gamma_T(T,T_a)-\gamma_\Gamma(\Gamma,\Gamma_0), \quad (1)$$

where $\gamma_0$ is the reference value of the surface tension, $\gamma_T = -\frac{\partial\gamma}{\partial T}\Big|\ T=T_a$ and $\gamma_\Gamma = -\frac{\partial\gamma}{\partial \Gamma}\Big|\ \Gamma=\Gamma_a$ For the sake of straightforwardness of this research and in order to preclude cumbersome algebra, let us accept that the quantities of the viscosity and density, as well as thermal conductivities, not alter with temperature field.

### 2.1 Governing Equations

The governing relations contain the continuity and Navier-Stokes equations for the flow of the liquid film and the energy equation for the temperature field. In two-dimensional form, the governing equations can be expressed as:

$$\frac{\partial u}{\partial x}+\frac{\partial v}{\partial y}=0, \quad (2)$$

$$\rho\left(\frac{\partial u}{\partial t}+u\frac{\partial u}{\partial x}+v\frac{\partial u}{\partial y}\right) = -\frac{\partial p}{\partial x}+\mu\left(\frac{\partial^2 u}{\partial x^2}+\frac{\partial^2 u}{\partial y^2}\right)+\rho g\sin\beta \quad (3)$$

$$\rho\left(\frac{\partial v}{\partial t}+u\frac{\partial v}{\partial x}+v\frac{\partial v}{\partial y}\right) = -\frac{\partial p}{\partial y}+\mu\left(\frac{\partial^2 v}{\partial x^2}+\frac{\partial^2 v}{\partial y^2}\right)-\rho g\cos\beta, \quad (4)$$

$$\rho c_p\left(\frac{\partial T}{\partial t}+u\frac{\partial T}{\partial x}+v\frac{\partial T}{\partial y}\right)=\kappa\left(\frac{\partial^2 T}{\partial x^2}+\frac{\partial^2 T}{\partial y^2}\right). \quad (5)$$

Here, $u$ and $v$ distinguish the components of the velocity vector $\mathbf{V}$, while $\rho$, $\mu$ and $p$ are density, dynamical viscosity, and the pressure respectively. In addition, $c_p$ denotes the heat capacity at the constant pressure and $\boldsymbol{\kappa}$ refers to the thermal conductivity of the fluid layer whereas $T$ denotes its temperature. Since the motion is supposed to be slow, the term due to the viscosity and the joule dissipation is ignored as they are really very small in creeping motion. The corresponding boundary conditions on the lower boundary and the free surface are added to achieve and complete the problem statement (2-5). On the solid lower plane substrate, $y = 0$, the no-slip, and the no-penetration constraints imposed for the velocity components and temperature field read

$$u=v=0, \quad T=T_w \quad (6)$$

At the free surface, the boundary constraints are respectively, the kinematic condition, surfactant equation as well as heat transfer governed by Newton's law of cooling. Across the interface, we have the of the normal component of the surface-traction that balanced by surface tension times curvature, which is expressed as

$$p_{air}-p+\left(\mu(\nabla\mathbf{V}+\nabla\mathbf{V}^{Tr}).\mathbf{n}\right).\mathbf{n}=-\gamma(\Gamma,T)\nabla.\mathbf{n}, \quad (7)$$

where $p_{air}$ represents the pressure afforded by the air, which is taken to be constant and $\boldsymbol{\nabla}\mathbf{V}^{Tr}$ is the transpose of the gradient of the velocity vector. At any point on the free surface, the unit out-ward normal vector is defined by $n=\nabla\,(y-[\ell+h(x,t)])/|\nabla\,(y-[\ell+h(x,t)])|$,

and $\mathbf{t}$ is the unit vector along the tangential direction at that point such that $\mathbf{n}\cdot\mathbf{t} = 0$. The tangential component of the stress tensor is affected by the air pressure and the Marangoni effects and reads as

$$\left(\mu(\nabla\mathbf{V}+\nabla\mathbf{V}^{Tr}).\mathbf{t}\right).\mathbf{n}=\nabla\gamma(\Gamma,T).\mathbf{t}+\tau_s \quad (8)$$

Expressing that the free surface is a material interface, the location of the interface can be founded by using the following kinematic term

$$\frac{\partial h}{\partial t}+\big((u,v).\nabla\big)(l+h-y)=0. \quad (9)$$

Newton's law of cooling at the interface $y = h(x,t)$ is given as

$$\kappa \nabla T.\mathbf{n} + qt = 0, \tag{10}$$

where $q$ is the coefficient of uniform heat transfer describing the rate transport of the temperature from the film to the surrounding air phase. For an insoluble surfactant, the distribution of the surface concentration $\Gamma(x,t)$ at the free interface of the liquid is governed by the transport relation (Frenkel and Halpern (2002), Pozrikidis (2003); Mikishev and Nepomnyashchy (2010)):

$$\frac{\partial (L\Gamma)}{\partial t} + \frac{\partial (L\Gamma u)}{\partial x} = D_s \frac{\partial}{\partial x}\left(\frac{1}{L}\frac{\partial \Gamma}{\partial x}\right). \tag{11}$$

Here, in this equation $L = \sqrt{1 + \left(\partial h/\partial x\right)^2}$ and $D_s$ is the surface diffusion coefficient. The influence of buoyancy can be ignored by the validity that $D_s$ is taken to be small enough. Indeed, it should be stated here, that the surfactants are the abbreviations of the underlined letters of the three words, "surface active agents", which are materials and chemicals (alcohols, fatty acids and some proteins are good examples for such materials) that tend to accumulate at surfaces or interfaces, causing changes in their behavior.

Now, in order to remove the units related to the above system involving the physical parameters, reference scales are specified. So we introduce the following quantities to form non-dimensional governing relations and boundary constraints:

$$(u,v) = U_c(\bar{u},\bar{v}), \quad (x,y) = l(\bar{x},\bar{y}), \quad t = \frac{l}{U_c}\bar{t},$$
$$p = \frac{\rho g l \sin\beta}{2}\bar{p}, \quad T = (T_w - T_a)\bar{T} + T_a, \quad \Gamma = \Gamma_0\bar{\Gamma} \tag{12}$$

where we select the unperturbed film thickness $\ell$ as the characteristic length and the basic surface velocity $U_c = \frac{\rho g \ell^2 \sin\beta}{2\mu}$ is used to scale the velocity components. Using these dimensionless quantities (dropping the bar sign for simplicity), the equations of motion and heat equation read

$$\frac{\partial u}{\partial x} + \frac{\partial v}{\partial y} = 0, \tag{13}$$

$$R_e\left(\frac{\partial u}{\partial t} + u\frac{\partial u}{\partial x} + v\frac{\partial u}{\partial y}\right) = -\frac{\partial p}{\partial x} + \frac{\partial^2 u}{\partial x^2} + \frac{\partial^2 u}{\partial y^2} + 2, \tag{14}$$

$$R_e\left(\frac{\partial v}{\partial t} + u\frac{\partial v}{\partial x} + v\frac{\partial v}{\partial y}\right) = -\frac{\partial p}{\partial y} + \frac{\partial^2 v}{\partial x^2} + \frac{\partial^2 v}{\partial y^2} - 2\cot\beta, \tag{15}$$

$$P_e\left(\frac{\partial T}{\partial t} + u\frac{\partial T}{\partial x} + v\frac{\partial T}{\partial y}\right) = \frac{\partial^2 T}{\partial x^2} + \frac{\partial^2 T}{\partial y^2}, \tag{16}$$

where, $P_e = P_r R_e$ is the Péclet number and $P_r = \frac{\mu c_p}{\kappa}$ denotes Prandtl number, $R_e = \frac{\rho \ell U_c}{\mu}$ refer to the Reynolds number. In terms of these non-dimensional parameters, the boundary conditions at the inclined substrate y = 0 then read

$$u = v = 0, \quad T = 1. \tag{17}$$

The interfacial stresses created, by the surface tension gradient including the Marangoni impacts and the related regimes of instability are known as thermocapillary instability. Hence, the boundary conditions at the free interface $y = h(x, t)$ can be written in the form

$$L^{-1}\left\{\left(\frac{\partial u}{\partial y} + \frac{\partial v}{\partial x}\right)\left(1 - \left(\frac{\partial h}{\partial x}\right)^2\right) + 2\left(\frac{\partial v}{\partial y} - \frac{\partial u}{\partial x}\right)\frac{\partial h}{\partial x}\right\} = -M_a\left(\frac{\partial T}{\partial x} + \frac{\partial T}{\partial y}\frac{\partial h}{\partial x}\right) - N_e\frac{\partial T}{\partial x} + \tau_s, \tag{18}$$

$$p_{air} - p + 2L^{-2}\left\{\frac{\partial v}{\partial y} + \frac{\partial u}{\partial x}\left(\frac{\partial h}{\partial x}\right)^2 - \left(\frac{\partial u}{\partial y} + \frac{\partial v}{\partial x}\right)\frac{\partial h}{\partial x}\right\} = L^{-3}\left\{\frac{1}{C_a} - M_a T - N_e(\Gamma - 1)\right\}\frac{\partial^2 h}{\partial x^2}, \tag{19}$$

$$\frac{\partial h}{\partial t} + u\frac{\partial h}{\partial x} - v = 0, \tag{20}$$

$$\frac{\partial (L\Gamma)}{\partial t} + \frac{\partial (L\Gamma u)}{\partial x} = \frac{1}{P_{es}}\frac{\partial}{\partial x}\left(\frac{1}{L}\frac{\partial \Gamma}{\partial x}\right) \tag{21}$$

$$L^{-1}\left(\frac{\partial T}{\partial y} - \frac{\partial h}{\partial x}\frac{\partial T}{\partial x}\right) + B_i T = 0, \tag{22}$$

where $M_a = \frac{\gamma_T (T_w - T_a)}{U_{c\mu}}$ denotes the Marangoni number, $N_e = \frac{\gamma_\Gamma \Gamma_0}{U_{c\mu}}$ is the elasticity number encapsulating the effect of surface surfactants, $C_a = \frac{\mu U_c}{\gamma_0}$ represents the capillary number that expresses the effect of surface tension, $P_{es} = \frac{\ell U_c}{D_s}$ is the surfactant Péclet number and $B_i = \frac{q\ell}{\kappa}$ refers to the Biot number, which measures the heat transfer mechanism at the free surface and if Bi equals zero, the surface is then thermally insulated.

## 2.2 Base State Solutions

In solving the steady unidirectional flow motion in the $x$ direction due to gravity field we get the base state solutions whose stability configuration is of interest in this work. That is, when the system is unperturbed, the heat distribution and the velocity range are separated from each other. Hence, to obtain the base state solutions of the velocity and the heat equation, we use the zero order of the governing equations and the associated boundary conditions. Hence the solutions of the basic pressure $p_0(y)$, velocity $(U_0(y), V_0(y))$ and the base heat $T_b(y)$ are given by

$$U_0(y) = (2y - y^2) + \tau_s y, \quad V_0(y) = 0,$$

$$p_0(y) = \hat{p}_0 + 2\cot\beta(1-y), \quad T_b(y) = 1 - \frac{B_i}{1+B_i} y. \quad (23)$$

Here it is noted that the basic state velocity profile is parabolic in y, while the unperturbed temperature is a linear function of $y$ alone and $\hat{p}_0$ represents the air constant pressure. Also, we note that while the basic velocity of the diffused surfactant is not affected, it is strongly affected by the shear stress imposed on the surface.

### 2.3 Linearization

In order to discuss the linear stability analysis, the velocities components, the pressure distribution, the temperature filed, the interfacial position, are perturbed about its equilibrium position as well as the diffusive surfactant by introducing infinitesimal perturbation and given by the relations

$$u = U_0 + u', \quad v = v', \quad p = p_0 + p',$$

$$T = T_b + T', \quad h = h', \quad \Gamma = 1 + \Gamma'. \quad (24)$$

By involving these quantities into the equations of motion, heat equation and linearizing them with respect to the base states, one can obtain

$$\frac{\partial u'}{\partial x} + \frac{\partial v'}{\partial y} = 0, \quad (25)$$

$$R_e\left(\frac{\partial u'}{\partial t} + U_0\frac{\partial u'}{\partial x} + v'\frac{\partial U_0}{\partial y}\right) = -\frac{\partial p'}{\partial x} + \frac{\partial^2 u'}{\partial x^2} + \frac{\partial^2 u'}{\partial y^2}, \quad (26)$$

$$R_e\left(\frac{\partial v'}{\partial t} + U_0\frac{\partial v'}{\partial x}\right) = -\frac{\partial p'}{\partial y} + \frac{\partial^2 v'}{\partial x^2} + \frac{\partial^2 v'}{\partial y^2}, \quad (27)$$

$$P_e\left(\frac{\partial T'}{\partial t} + U_0\frac{\partial T'}{\partial x} + v'\frac{\partial T_b}{\partial y}\right) = \frac{\partial^2 T'}{\partial x^2} + \frac{\partial^2 T'}{\partial y^2}, \quad (28)$$

which are called as the perturbation relations. At this point, it is appropriate to call a perturbed stream function from the perturbed continuity equation such that $u' = \partial\psi'/\partial y$ and $v' = \partial\psi'/\partial x$. To discuss the stability process of the liquid film, the normal mode is investigated by supposing the traveling wave solutions:

$$(\Psi', p', T', h', \Gamma') = \left(\hat{\phi}(y), \hat{p}(y), \hat{T}(y), \hat{h}, \hat{\Gamma}\right)\exp[ik(x-ct)], \quad (29)$$

where k denotes the wave number of the disturbance and
$c = c_r + ic_i$ represents the velocity of complex wave. Here the wave number $k$ is taken to be real and the letter $i$ indicates $\sqrt{-1}$, the imaginary number. The imaginary part of $c$ gives the growth rate $s = kc_i$, while the phase velocity of the corresponding infinitesimal perturbations is determined by $c_r$. The system is unstable (stable) when $s$ is negative (positive) and when $s = 0$, the system is neutrally stable. Substituting the perturbed variables into relations (26)-(28) and removing the pressure term, thus we can obtain the equations governing the linear stability system as

$$\frac{d^4\hat{\phi}}{dy^4} - 2k^2\frac{d^2\hat{\phi}}{dy^2} + k^4\hat{\phi} = ikR_e\left\{(U_0 - c)\left(\frac{d^2\hat{\phi}}{dy^2} - k^2\hat{\phi}\right) - \frac{d^2U_0}{dy^2}\hat{\phi}\right\}, \quad (30)$$

$$\frac{d^2\hat{T}}{dy^2} - k^2\hat{T} = ikP_e\left\{(U_0 - c)\hat{T} - \frac{dT_b}{dy}\hat{\phi}\right\}. \quad (31)$$

Eq. (30) is in the form of Orr-Sommerfeld equation (Wei (2004), Samanta (2008a)). The disturbance stream function $\hat{\phi}$ and the heat $\hat{T}$ are subject to the boundary constraints at the plate and at the free surface. Thus, the linearized boundary conditions at the plane ($y = 0$) become

$$\hat{\phi}(0) = \frac{d\hat{\phi}(0)}{dy} = 0, \quad (32)$$

$$\hat{T}(0) = 0, \quad (33)$$

while the boundary conditions at the free surface (y = 1) read

$$\frac{d^2\hat{\phi}(1)}{dy^2} + k^2\hat{\phi}(1) + \hat{h}\frac{d^2U_0(1)}{dy^2} + ik\left\{N_e\hat{\Gamma} + M_a\left(\hat{T}(1) + \frac{dT_b(1)}{dy}\hat{h}\right)\right\} = 0, \quad (34)$$

$$\frac{d^3\hat{\phi}(1)}{dy^3} - 3k^2\frac{d\hat{\phi}(1)}{dy} + ikR_e\left\{\frac{dU_0(1)}{dy}\hat{\phi}(1) + (c - U_0(1))\frac{d\hat{\phi}(1)}{dy}\right\} - ik\hat{h}\left\{2\cot\beta + k^2\left(\frac{1}{C_a} - M_aT_b(1)\right)\right\} - 2k^2\hat{h}\frac{dU_0(1)}{dy} = 0, \quad (35)$$

$$\hat{\phi}(1) - (c - U_0(1))\hat{h} = 0, \quad (36)$$

$$\frac{d\hat{\phi}(1)}{dy} + \frac{dU_0(1)}{dy}\hat{h} - (c - U_0(1))\hat{\Gamma} = 0, \quad (37)$$

$$\frac{d\hat{T}(1)}{dy} + B_i\left\{\hat{T}(1) + \frac{dT_b(1)}{dy}\hat{h}\right\} = 0. \quad (38)$$

Here, in driving Eq. (35), we use the linearized version of the normal stress equation (19), by removing ing the pressure value depending on the stream function via the $x$−momentum relation (26). Further, all the physical variables are developed about the surface y =1 in terms of Taylor expansion.

## 3. STABILITY ANALYSIS

For each $k$, the system of (30) and (31) with related boundary conditions assigns an eigenvalue system that can be utilized to get the wave velocity $c$, that is a complex value. Indeed, for arbitrary Re and k, there

are no analytical exact solutions for such a system and so numerical estimations must be used to solve the stability picture in general. In this section, we will deal with these equations in two cases, the first is the situation of low Reynolds number i.e. $R_e \ll 1$, in which that the inertial forces will be small compared to the viscous forces (which is known by Stokes approximation). The second is the long waves evolution, in which we consider low wave number $k \to 0$, thus an asymptotic analysis in the small parameter $k$ is possible, which yields an exact expression for the wave velocity as an asymptotic series in $k$ (Kwak and Pozrikidis (2001), Shankar (2005), Gao and Lu (2007); Barra *et al*.(2019)).

### 3.1 Stokes Flow

For an extreme example, it is interesting to study the inertialess stability and let the Reynolds number be zero, and consequently, $P_e = R_eP_r$ is also led to zero. Thus, it is easy to find the general solution of the system (30) and (31) in the Stokes flow:

$$\hat{\phi}(y) = A_1e^{ky} + A_2e^{-ky} + A_3ye^{ky} + A_4ye^{-ky}, \tag{39}$$

$$\hat{T}(y) = B_1e^{ky} + B_2e^{-ky}. \tag{40}$$

From the boundary conditions, we once more obtain a secular equation by setting the determinant of the coefficients of $A's$, $B's$, $\hat{h}$ and $\hat{\Gamma}$ to zero:

$$A = \begin{vmatrix} 1 & 1 & 0 & 0 \\ k & -k & 1 & 1 \\ -2k^2e^k & 2k^2e^{-k} & -2k^2e^k & 2k^2e^{-k} \\ 2k^2e^k & 2k^2e^{-k} & 2k(k+1)e^k & 2k(k-1)e^{-k} \\ ke^k & -ke^{-k} & (1+k)e^k & (1-k)e^{-k} \\ e^k & e^{-k} & e^k & e^{-k} \\ 0 & 0 & 0 & 0 \\ 0 & 0 & 0 & 0 \end{vmatrix}$$

$$\begin{vmatrix} 0 & 0 & 0 & 0 \\ 0 & 0 & 0 & 0 \\ 0 & 0 & \tilde{\tilde{h}} & 0 \\ iM_ake^k & iM_ake^{-k} & iM_a\bar{T}_b' + \bar{U}_0'' & ikN_e \\ 0 & 0 & \bar{U}_0' & U_{p_e} \\ 0 & 0 & \bar{U}_0' - c & 0 \\ 1 & 1 & 0 & 0 \\ B_i(1+k)e^k & B_i(1-k)e^{-k} & B_i\bar{T}_b' & 0 \end{vmatrix}$$

where $\tilde{\tilde{h}} = -2i\cot\beta - ik^2(\frac{1}{C_a} - M_a\overline{T}_b) - 2k\overline{U_0}$, and $U_{pe} = \overline{U_0} - \frac{ik}{p_{es}} - c$. Here, and in what follows, for simplicity we write $U_0(1) = \overline{U_0} = 1 + \tau_s$, $\frac{dU_0(1)}{dy} = \overline{U_0'} = \tau_s$, $\frac{d^2U_0(1)}{dy^2} = \bar{U}_0'' = -2$, $T_b(1) = \overline{T}_b$ and $\frac{dT_0(1)}{dy} = \bar{T}_0'$.

Direct computation of this determinant gives the dispersion relation of the Stokes flow:

$$\alpha_0c^2 + (\alpha_1 + i\alpha_2)c + \alpha_3 + i\alpha_4 = 0, \tag{41}$$

where the quantities $\acute{\alpha}$ s are obvious from the context. This equation may be used to discuss the stability of Stokes flow, in the presence of all physical parameters acted on the problem at hand. Applying the Routh-Hurwitz stability criterion (Pop and Ingham (2001); El-Sayed (2013)) to Eq. (41), we can check the signs of the real parts of these roots without getting them explicitly, and hence the necessary and sufficient terms for stability are

$$\alpha_2 > 0, \quad \chi = \alpha_3\alpha_2^2 - \alpha_1\alpha_2\alpha_4 + \alpha_0\alpha_4^2 \le 0. \tag{42}$$

Note that, the quadratic dispersion relation (41), in the limiting case clean flow (i.e. no insoluble surfactants at the free surface) reduces to linear dispersion equation in c. Thus the phase speed and the growth rate corresponding to the Stokes clean flow are given by

$$c_r = \frac{k\bar{U}_0'' - (2k - \sinh 2k)\bar{U}_0'}{k(1 + 2k^2 + \cosh 2k)} - \bar{U}_0, \tag{43}$$

$$\begin{aligned} kc_i = &\left\{16k^3(1 + 2k^2 + \cosh 2k)(k\cosh k \right. \\ &\left. + B_i\sinh k)\right\}^{-1}\left\{\frac{8k^2}{C_a}(2k - \sinh 2k)(k\cosh 2k \right. \\ &\left. + B_i\sinh 2k)\left[k^2(C_aM_a\bar{T}_b - 1) - 2C_a\cot\beta\right]\right. \\ &\left. + 16M_ak^6\cosh k\bar{T}_b'\right\}. \end{aligned} \tag{44}$$

It is illustrated from Eq. (43) that phase velocity of the infinitesimal disturbance is dependent directly on the shear stress offered by air and independent of the thermocapillary parameters. In addition, in the situation when the imposed shear is put to be zero (i.e. $\tau_s = 0$), Eqs. (43) and (44) are then coincide with that obtained by Samanta (2008a).

In Figs. 2 through 4, our main aim is to observe the effects of several values included in the analysis on the linear stability criterion of the system under consideration, in the limit of Stokes flow. In order to show this examination, numerical values for the stability relation (42) are achieved by the variation of the physical terms. The first condition of (42) is always satisfied when $\beta < \pi/2$. Therefore, the stability configuration can be controlled only by the second condition in relation (42). Hence, the stability pictures occur when $\chi < 0$, otherwise, instability holds when $\chi > 0$.

The graphs displayed in part (a) of Fig. 2 show variation of the condition $\chi$ with the imposed shear stress $\tau_s \in (-3,3)$, for different values of the surfactant Péclet number $P_{es}$, and the other parameters are held fixed as $\beta = \pi/4$, $k = 0.1$, $B_i = 2$, $C_a = 2$, $M_a = 3$, and $N_e = 2$. It is clear from this figure that the condition $\chi > 0$ is satisfied when $\tau_s < -2$ and hence the system is unstable, afterwards the system is stable ($\chi < 0$). In addition, it is observed that there are three distinct values $\tau_s = 0.65$, 1 and 2 corresponding to three values of $P_{es} = 1.5$, 1 and 0.5, after which the motion resumes again unsettled. Therefore, we conclude, in the case of Stokes flow, that the surfactant Péclet number has destabilizing impacts since the critical stress decreases by increasing the Péclet number values.

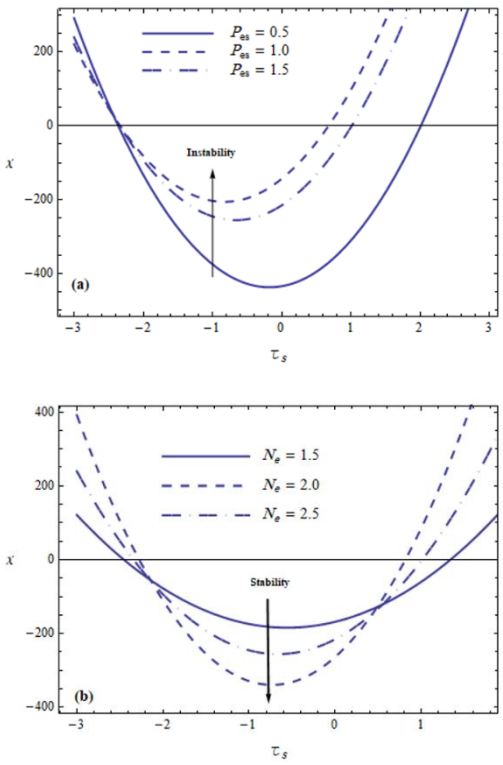


**Fig. 2. The graph construction is based on the stability condition (42) in the plane ($\chi - \tau_s$) for a system having $\beta = \pi/4$, $k = 0.1$, $B_i = 2$, $C_a = 2$, $M_a = 3$: Part (a) show the variation of the surfactant Péclet number Pes, Part (b) illustrate the effect of elasticity parameter Ne.**

Fig. 2(b) depicts the stability curves obtained from the second condition of (42) versus the shear stress parameter axis and different elasticity numbers, for the same parameters considered in Fig. 2(a) with $P_{es}$=1. As shown in Fig. 2(b) with increasing in $N_e$ = 1.5, 2 and 2.5 for the solid, dotted-dashed and broken lines respectively, the stability curves shift to the lower region $\chi < 0$, i.e., the higher $N_e$, the more negative parameter $\chi$. Hence, the elasticity parameter is found to have stabilizing effects in the movement of the free surface. Further, in point of view the horizontal axis ($\tau_s$ −axis), it is worth mentioning to observe that, when the values of the elasticity parameter increased the width of the corresponding curve is narrowed. In other words, the distance in the range $\tau_s$ between the two intercepted points for each curve is contracted due to increase in the elasticity parameter. That is the size of the range $\tau_s$ −axis narrower for higher $N_e$ and wider for lower $N_e$, which show a destabilizing influence of the imposed shear stress $\tau_s$ (this behavior of $\tau_s$ will be confirmed in the discussion of Fig. 4(a) below).

The examination of change of the Marangoni and Biot numbers in the stability criteria is shown in the ($\chi - \tau_s$) plane via the parts (a) and (b) of Fig. 3. The graph illustrated in this figure is carried out for three distinct values of $M_a$ (= 5, 10, 15) and $B_i$ (= 1, 1.5, 2) for the parts (a) and (b) respectively. It can be seen from the part (a) of Fig. 3 that the stability domains above the transition curves and under the $\tau_s$ −axis are contracted due to the increase of Ma, that is when $\tau_s < 0$, and hence the Marangoni number has a destabilizing effect on the movement of the fluid film. In a similar manner to that discussed in Fig. 2(b), the inspection of part (b) of Fig. 3 illustrates that the regular regions under the lines are increased when the Biot number increases. This reveals that the Biot number has a stabilizing impact on the movement of the fluid layer.

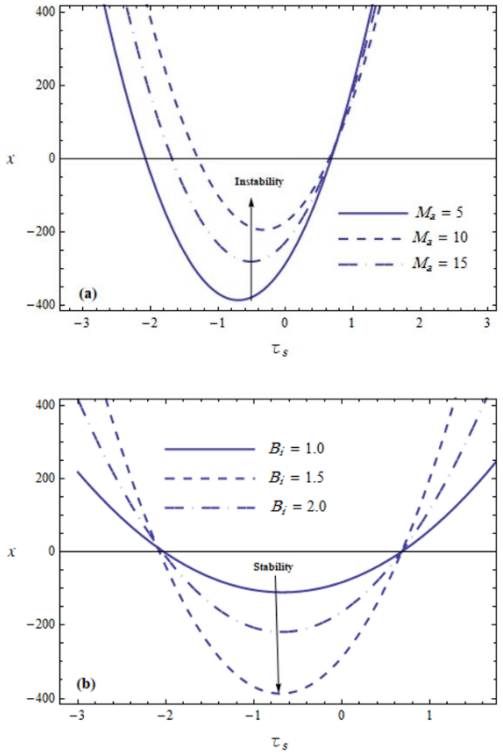


**Fig. 3. The condition $\chi$ as a function of the imposed shear stress, for a system having the same physical parameters as imposed in Fig. 2: Part (a) shows the impact of the Marangoni number, Part (b) investigate the role Biot number.**

In order to study the mechanism of the stabilization of the imposed shear stress and the capillary number on the film flow, Fig. 4 is illustrated in which the condition $\chi$ is plotted against the dimensionless wave number $k$, for $M_a$=50, $B_i$=0.2, $N_e$=2 and $P_{es}$=2. In part (a) of this graph, by in-creasing the imposed shear $\tau_s$ =−1, 0, 1, it is noted that the unstable wavenumbers field enlarged. Therefore, we conclude the imposed shear stresses have destabilizing behavior since the critical wave numbers stretch by increasing the shear parameter quantity.

On the other hand, it is worth mentioning to observe that the imposed shear destabilizes the motion when it flows in the direction of $x$−axis (downhill, $\tau_s > 0$) and decreases the stability threshold (compared to the situation when $\tau_s = 0$). Further, when the imposed shear acted against the direction of x−axis (uphill, $\tau_s < 0$), the flow regime is better stabilized than when $\tau_s = 0$. A similar result was reported by Iqbal (2013), in his studies of stability and dynamics for air-aided shear on a thin layer displayed to a constant magnetic

range. Increasing the value of the capillary number stepwise from 3 to 7 is presented in the second part of Fig. 4. It is clear from this figure that increasing the capillary number results in increasing the cutoff wave number, in addition decreasing the firm areas under the curves. It is apparent from this discussion that the variation of the capillary number plays a destabilizing role in the motion of the fluid thin film. Since the surface tension is related conversely with the capillary number, thus we deduce that the surface tension has a stabilizing behavior.

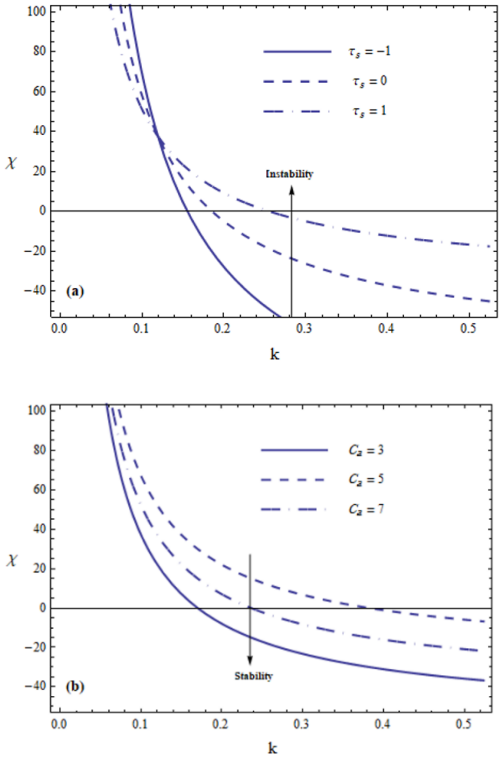


**Fig. 4. The graph building is based on the stability conditions (42) in the plane ($\chi - k$): Part (a) discuss the influence of the considered shear stress, Part (b) displays the influence of the capillary number.**

## 3.2 Long Waves Approximation

In this part, we consider the effect of Reynolds number on the linear stability issue for the general form of Orr-Sommerfeld and energy equations. In this case, we apply the long-wavelength solutions where a regular perturbation technique is used (Tseluiko and Papageorgiou (2006), Sadiq, *et al.*(2010), Zakaria (2012), Merkt, *et al.* (2015), Alkharashi *et al*. (2019); Alkharashi (2019)). Thus the appropriate long wave motion is

$$\left.\begin{aligned}
\hat{\phi} &= \hat{\phi}_0 + k\hat{\phi}_1,\\
\hat{T} &= \hat{T}_0 + k\hat{T}_1,\\
\hat{h} &= \hat{h}_0 + k\hat{h}_1,\\
\hat{\Gamma} &= \hat{\Gamma}_0 + k\hat{\Gamma}_1,\\
\hat{c} &= \hat{c}_0 + k\hat{c}_1,.
\end{aligned}\right\} \tag{45}$$

By achieving the regular perturbation mode, by inserting expansions (45) into Eqs. (30)-(38), and combine the terms in each order of k, we gain the following arranged problems and their related solutions. At order $O(1)$ yields

$$\frac{d^4\hat{\phi}_0(1)}{dy^4} = 0, \qquad \frac{d^2\hat{T}_0(1)}{dy^2} = 0, \tag{46}$$

$$\hat{\phi}_0(0) = \frac{d\hat{\phi}_0(0)}{dy} = 0, \quad \hat{T}_0(0) = 0, \tag{47}$$

$$\frac{d^2\hat{\phi}_0(1)}{dy^2} + \hat{h}_0 U_0'' = 0, \tag{48}$$

$$\frac{d^3\hat{\phi}_0(1)}{dy^3} = 0, \tag{49}$$

$$\hat{\phi}_0(1) - \left(c_0 - \bar{U}_0\right)\hat{h}_0 = 0, \tag{50}$$

$$\frac{d\hat{\phi}_0(1)}{dy} + \hat{h}_0\bar{U}_0' - \left(c - \bar{U}_0\right)\hat{\Gamma}_0 = 0, \tag{51}$$

$$\frac{d\hat{T}_0(1)}{dy} + B_i\hat{T}_0(1) + B_i\bar{T}_b'\hat{h}_0 = 0. \tag{52}$$

The solution to (46) that satisfies (47)-(52) can take the form

$$\hat{\phi}_0 = -\frac{1}{2}\bar{U}_0''\hat{h}_0 y^2, \qquad \hat{T}_0 = \bar{T}_b'^2\hat{h}_0 y. \tag{53}$$

Substituting Eq. (53) into (50) and (51) we get, respectively,

$$\{c_0 - \bar{U}_0 + \frac{1}{2}\bar{U}_0''\}\hat{h}_0 = 0, \tag{54}$$

$$\{\bar{U}_0' - \bar{U}_0''\}\hat{h}_0 - \{c_0 - \bar{U}_0\}\hat{\Gamma}_0 = 0. \tag{55}$$

In the absence of heat transfer, the above linear system is closed to the problem considered by Bhat and Samanta (2019). For dealing with this system, we have two temporal modes as illustrated by (Kwak and Pozrikidis (2001); Wei (2004)), the first is the interface mode ($\hat{h}_0 \neq 0$, $\hat{\Gamma}_0 \neq 0$), this mode is caused by the surface deflections via the validity of leading-order kinematic relation (54) gives $c_0$ (as in free-falling films). Thus $c_0$ and $\hat{\Gamma}_0$ are defined by

$$c_0 = 1 + \bar{U}_0 = 2 + \bar{U}_0', \tag{56}$$

and hence leading order amplitude of the surfactant reads

$$\hat{\Gamma}_0 = \frac{(\bar{U}_0' - \bar{U}_0'')\hat{h}_0}{c_0 - \bar{U}_0} = (2 + \bar{U}_0')\hat{h}_0. \tag{57}$$

Noting that in Eq. (56) $\overline{U_0}$= 1 + $\tau_s$ this eluci-dated that in the surface mode the phase velocity is strongly affected by the imposed shear stress. Furthermore, in view of Eq. (57) the deformation of the free surface affects the surfactant concentration that perturbed on it. In addition, from this equation, the concentration of insoluble surfactants is in (out) phase with the

interface when $2 + \overline{U_0} > 0 (< 0)$. Without necessarily having a surface deflection, the second type is the surfactant mode that can be ex-cited by the perturbations of the surfactant amount that concentrated at the free surface $\hat{\Gamma}_0 \neq 0$. Thus for this mode, we have

$$\hat{h}_0 = 0, \quad c_0 = \bar{U}_0. \tag{58}$$

In comparing Eqs. (56) and (58), we see at the free surface, that the leading order surfactant mode movies with the same speed of the liquid thin layer, while the leading order surface mode exceeds by the unity. This means that the leading order surface mode movies faster than the leading order surfactant behavior. On the other hand, in the existence of insoluble surfactants in this work, our asymptotic study investigates that at leading order, c0 is identified from the leading order surfactant relation (54) which is purely real and is concur to the results by Shankar (2005). In other words, the impacts of surfactants and heat do not show at the leading order problem $O(1)$ and hence does not give to the system's stability. Thus, in order to discuss the stability of the problem, one must determine the first correction of c1, which is obtained by solving the problem at order $O(k)$. At the $O(k)$ problem, we obtain the next relation:

$$\frac{d^4\hat{\phi}_1(y)}{dy^4} + iR_e\left\{(c - U_0(1))\frac{d^2\hat{\phi}_0(y)}{dy^2} + \frac{d^2U_0(y)}{dy^2}\hat{\phi}_0(y)\right\} = 0, \tag{59}$$

$$\frac{d^4\hat{T}_1(y)}{dy^4} + iP_e\left\{(c_0 - U_0(1))\hat{T}_0 + \frac{d^2\hat{T}_b(y)}{dy^2}\hat{\phi}_0(y)\right\} = 0, \tag{60}$$

$$\hat{\phi}_1(0) = \frac{d\hat{\phi}_1(0)}{dy} = 0, \qquad \hat{T}_1(0) = 0, \tag{61}$$

$$\frac{d^2\hat{\phi}_1(1)}{dy^2} + \hat{h}_1\bar{U}_0'' + i\{M_a(\hat{T}_0(1) + \hat{h}_0\bar{T}_b') + N_e\hat{\Gamma}_0\} = 0, \tag{62}$$

$$\frac{d^3\hat{\phi}_1(y)}{dy^3} - 2i\cot\beta\hat{h}_0 + iR_e\left\{(c - \bar{U}_0)\frac{d\hat{\phi}_0(1)}{dy} + \bar{U}_0'\hat{\phi}_0(1)\right\} = 0, \tag{63}$$

$$\hat{\phi}_1(1) - c_1\hat{h}_0 - (c_0 - \bar{U}_0)\hat{h}_1 = 0, \tag{64}$$

$$\frac{d\hat{\phi}_1(1)}{dy} - (c_0 - \bar{U}_0)\hat{\Gamma}_1 + (ip_{es}^{-1} + c_1)\hat{\Gamma}_0 + \hat{h}_1\bar{U}_0' = 0, \tag{65}$$

$$\frac{d\hat{T}_1(1)}{dy} + B_i\left(\bar{T}_b'\hat{h}_1 + \hat{T}_1(1)\right) = 0. \tag{66}$$

It should be observed from the above analysis that the influence of the capillary number expressing the impact of surface tension is investigated only in the Stokes flow. But in long wave approximation, the effect of capillary number manifests at the higher-order $O(k^3)$, which reveals that it does not contribute the long wave study but has a good influence in stabilizing short wave limit. The solution to (59) that satisfies (61)-(63) is taken the form

$$\hat{\phi}_1(y) = a_1y^3 + a_2y^2 - iR_e\hat{h}_0\left\{\frac{1}{120}(\bar{U}_0' - \bar{U}_0'')y^5 - \frac{c_0}{24}y^4\right\}, \tag{67}$$

where,

$$a_1 = \frac{i\hat{h}_0}{3}\cot\beta,$$

$$a_2 = -\frac{1}{2}\left[iN_e\hat{\Gamma}_0 + iM_a\hat{T}_0(1) + \hat{h}_1\bar{U}''\right] - \hat{h}_0\left\{i\cot\beta + \frac{1}{2}iM_a\bar{T}_b' - \frac{1}{12}iR_e\bar{U}_0''\left[6 - 3c_0 + \bar{U}_0' + 2\bar{U}_0''\right]\right\}.$$

In addition, the solution to (60) that satisfies (61) and (66) is given by

$$\hat{T}_1(1) = b_1y - \frac{i}{12}P_e\hat{h}_0\bar{T}_b'\left\{\frac{3}{5}P_e\bar{T}_b'y^5 + ((\bar{U}_0'' - \bar{U}_0')\bar{T}_b' - \frac{1}{2}\bar{U}_0'')y^4 + 2c_0\bar{T}_b'y^3\right\}, \tag{68}$$

where,

$$b_1 = \frac{iP_e\hat{h}_0}{60B_i}\left\{B_i\left(5\bar{U}_0' - 10c_0 - 7\right) + 5\left(4\bar{U}' - 6c_0 + 5\right)\right\}\bar{T}_b'^3 + \left\{\hat{h}_1 + \frac{i()P_e\hat{h}_0\bar{U}_0''}{24b_1}\right\}\bar{T}_b'^2.$$

As a special case of our model, when no heat transfer, the system is reduced to Eq. (67) only, in which a similar equation is in the model given by Bhat and Samanta (2019). In the following the surface and the surfactant modes will be discussed in terms of the first-order wave speed $c_1$

### 3.2.1 The interface Mode

As in the $O(1)$ approximation, we use $O(k)$ kinematic condition (64) to determine the c1 for the interface mode. So, by Substituting (67) into (64), with the help of (57), we obtain

$$c_1 = \frac{4}{15}iR_e\left(2 + \bar{U}_0'\right) - \frac{1}{2}iN_e\left(2 + \bar{U}_0'\right) - \frac{1}{2}iM_a\bar{T}_b'\left(1 + \bar{T}_b'\right) - \frac{2}{3}i\cot\beta. \tag{69}$$

The first term of Eq. (69) due to the inertial influence, has a stabilizing role if $2 + \overline{U_0} < 0$, that is, as the supposed shear ($\tau_s = \overline{U_0}$) expressible versus the gravity force is sufficiently strong. The second term

shows the impact of surfactant, which can stabilize the system as in the equilibrium state of flows under gravity domain (Wei (2004); Shankar (2005)) or destabilize due to the assumed shears with $\bar{U}_0' = \tau_s (< 0)(> 0)$. The third term is due to the Marangoni effects, which will be discussed numerically later. The last term represents the stabilizing effect due to the gravity field.

### 3.2.2 The Surfactant Mode

As mention above in the case of surfactant mode, we substitute Eq. (58) into Eq. (67), once obtain

$$\hat{\phi}_1 = -\frac{1}{2}\left\{iN_e\hat{\Gamma}_0 - \bar{U}_0''\hat{h}_1\right\} y^2. \tag{70}$$

In addition, by using Eq. (54) into Eq. (61), yields

$$iN_e\hat{\Gamma}_0 = -\bar{U}_0''\hat{h}_1. \tag{71}$$

This implies that

$$\hat{\phi}_1 = 0. \tag{72}$$

Eq. (72) for the surfactant, mode means that there is no flow at $O(k)$. As given in $O(1)$ issue, the $c_1$ for the diffuse surfactant mode is obtained by the O($k$) surfactant relation Eq. (65). By substituting Eq. (71) in Eq. (65), we have

$$c_1 = -\frac{-i(N_e\bar{U}_0' + P_{es}^{-1}\bar{U}_0'')}{\bar{U}_0''} = \frac{i}{2}(N_e\bar{U}_0' - 2P_{es}^{-1}). \tag{73}$$

Since from the assumption that $c = c_r + ic_i = c_0 + kc_1$, we conclude that the system is stable (unstable) if $Im(c_1) < 0$ ($> 0$). Thus from Eq. (69), the system is stabilized if $\bar{U}_0' > \frac{2}{N_e P_{es}}$ and the motion will be destabilized if $\bar{U}_0' > \frac{2}{N_e P_{es}}$. In addition, we note that for the insoluble surfactant when surface diffusion is supposed to be ignored $D_s = 0$, the system is stable (unstable) if $\bar{U}_0' < 0$ ($> 0$), which coincide with the result given by Wei (2004). It is apparent from Eq. (73) that when there is no imposed shear stress, the surfactant mode is then switched off and the only affected mode in this case is the interface mode (Kwak and Pozrikidis (2001), Wei (2004); Iqbal (2013)).

## 3.3 Marginal State Representation

In this section, our main purpose is to illustrate the impact of such physical dimensionless numbers as Marangoni, elasticity and Reynolds numbers on the stability process in the concept of neutral curves. In the marginal state, the neutral lines split up stable motion from the unstable ones. Mathematically, the neutral instability line is acquired by performing the constraints of stability for the linear growth rate of $Im(c_1) = 0$. As a condition of the instability of surfactant mode is obtained from Eq. (73), so that

$$\frac{\tau_s}{s}N_e - \frac{1}{P_{es}} > 0 \tag{74}$$

in which positive growth rate occurs, due to the presence of the shear stress that imposed at the surface. That is in the marginal state the critical value of the surfactant Péclet number is given by

$$P_{es_c} = \frac{2}{\tau_s N_e}. \tag{75}$$

It is obvious from Eq. (75) that the critical surfactant Péclet number is depending only at the surface surfactant, and the imposed shear stress, while the Reynolds number does not play any role in the surfactant mode. However, the system will grow exponentially with time and the surfactant mode becomes unstable if $P_{es} > P_{esc}$.

In the interface mode Eq. (69) is involved to obtain exact analytical expressions of the critical Marangoni, elasticity and Reynolds numbers, which outlined respectively as

$$M_{ac} = \frac{\{20\cot\beta + (15N_e - 8R_e)(2+\tau_s)\}}{15B_i(1+B_i)^{-2}}, \tag{76}$$

$$\begin{aligned} N_{ec} = \frac{1}{15((1+B_i)^2(2+\tau_s)}\Big\{&\big(8R_e(2+\tau_s) \\ &- 20\cot\beta\big)B_i^2 + (10R_e(2+\tau_s) - 40\cot\beta \\ &+15M_a)B_i - 20\cot\beta + 8R_e(2+\tau_s)\Big\}, \end{aligned} \tag{77}$$

$$\begin{aligned} R_{ec} = \frac{5}{8(1+B_i)^2(2+\tau_s)}\Big\{&\big(4\cot\beta + N_e(2+\tau_s)\big) \\ &\times B_i^2 + \big(8\cot\beta - 3M_a + 6N_e(2+\tau_s)B_i\big) \\ &+4\cot\beta + 3N_e(2+\tau_s)\Big\} \end{aligned} \tag{78}$$

In the limiting case of $M_a \to 0$, $\tau s \to 0$, and $B_i \to 0$, the critical Reynolds number Rec coincides with that mentioned in paper Blyth and Pozrikidis (2004), while as $N_e \to 0$ i.e., there is no insoluble surfactants contaminated the surface of the film we reached the result of Smith (1990) and Samanta (2014). Furthermore, in the absence of heat transfer, it recovers the result reported by Bhat and Samanta (2019). In Figs. 5-7, numerical calculations for Eqs. (76)-(78) are made to illustrate the graphical results for the marginal curves which separate the firm regions from the unsettled motions. That is the area below each curve of these figures satisfied the condition $Im(c_1) < 0$, and hence it represents stable regions. On the other hand the relation $Im(c_1) > 0$ is satisfied in the planes above each line of these graphs and thus we have unstable modes. Fig. 5(a) illustrates the neutral stability curves for the case of $\beta = \pi/4$, $\tau_s = 3$ and $R_e = 2$ and several values of elasticity number $N_e = 0.9$, 1, 1.1 and 1.2. It is worth mentioning to observe that the increase of $N_e$ quantity leads to a shrinkage of the area of unstable long wave case. Thus, the effect of increasing elasticity parameter or surfactant is to stabilize the fluid motion. On the other hand, in view of the horizontal axis of the Biot number, it obvious that at any one of the four neutral curves, when the Biot number increases, this leads to an extension in the regular area below the curve, which confirms the stabilizing influence of the Biot number obtained before in the case of stokes flow.

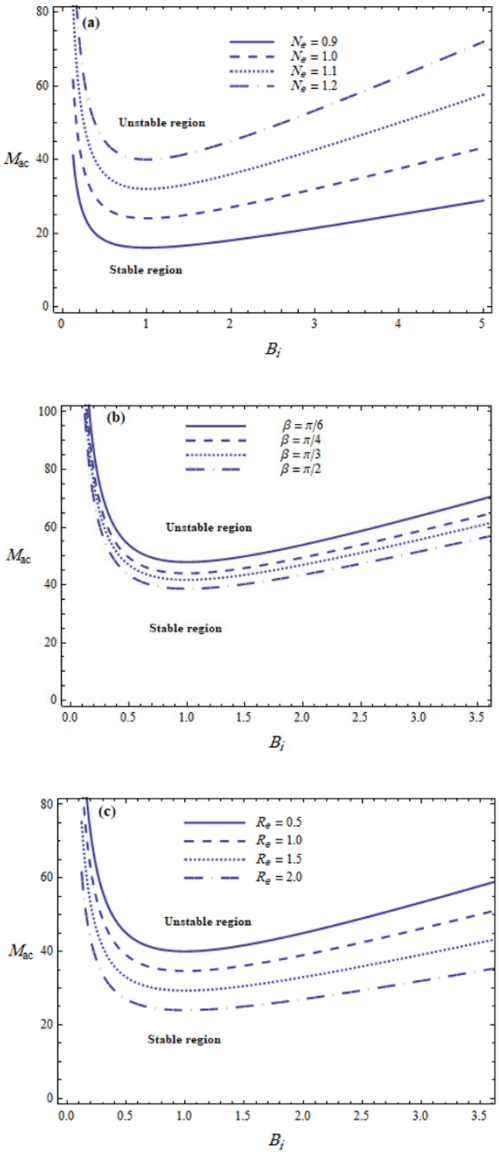


**Fig. 5. Neutral lines in the $M_{ac} - B_i$ plane for a system having the parameters β = π/4, $\tau_s$ = 3: Part (a) variation of $N_e$, with $R_e$ = 2, Part (b) changing of β, with $N_e$ = 3, Part (c) variation of $R_e$, with $N_e$ = 2.**

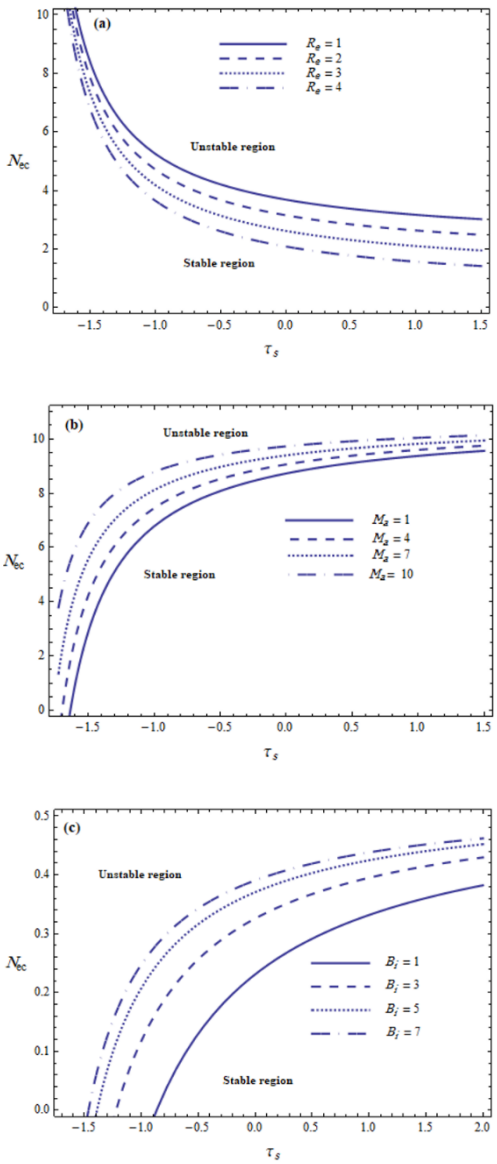


**Fig. 6. Critical elasticity parameter $N_{ec}$ to long wave versus the shear stress $\tau_s$, for a system having the same physical parameters as mentioned in Fig. 5 with $B_i$ = 2 Part (a) changing in $R_e$, with $M_a$ = 20, Part (b) variation of $M_a$, with $R_e$ = 3, Part (c) alteration of $B_i$, with $M_a$ = 2.**

Fig. 5(b) shows the marginal stability curves for several values of the angle of inclination at the same system considered in Fig. 5(a), where β = π/6, π/4, π/3 and π/2 corresponding to the solid, dashed, dotted and dotted-dashed curves respectively. It can be observed that increasing values of the angle of inclination have a destabilizing effect. In part (c) of the graph 5, the behavior of the critical Marangoni number is illustrated as a function of the Biot number for several values of the Reynolds number. It is clear that the increase of Reynolds number values lead to an extension of the region of a skittish long wave, which shows that the Reynolds number has a destabilizing effect on the motion of the interfacial waves based on the selected values of the physical parameters.

In Fig. 6, the plane ($N_{ec} - \tau_s$) through the parts (a-c) is divided by the neutral lines to regular and unsteady regions which are achieved by the validity of the factor $Im(c_1)$= 0. In part (a) of this graph the values 1, 2, 3 and 4 are selected for Reynolds number correspond to the continuous, dashed, dotted and dashed-dotted curves respectively. It is evidenced by the inspection of Fig. 6(a), for the previous input parameters, the critical elasticity number and the shear-imposed stress decreased as the Reynolds number increased, this shows that an increase in the Reynolds number has a destabilizing effect. The examination of change of the Marangoni number in the stability domain is shown in Fig. 6(b), when the values of the Marangoni number are increased from 1 to 10 for the sake of comparison.

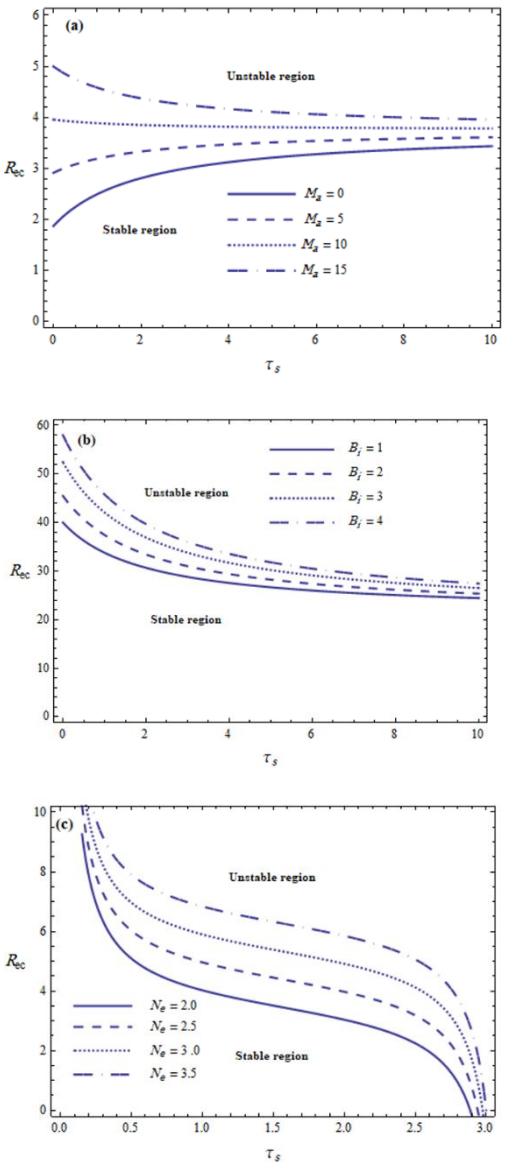


**Fig. 7. The graph is drawn for $R_{ec}$ versus $\tau_s$, according to the transition lines given from condition (78), for the same system set in Fig. 5, where variation of $M_a$, $B_i$ and $N_e$ for the partition (a), (b) and (c) respectively.**

It is observed that increasing Marangoni number results in increasing the firm areas under the curves, which stabilizes the system in turn confirms the significantly stabilizing influence of Marangoni number. Fig. 6(c) represents the neutral stability, when the values of the Biot number are stepwise increased from 0.1 to 0.7 for the sake of comparison. It is observed that increasing the Biot number results in decreasing the unsteady areas above the curves, which stabilizes the motion of the film. On the other hand, since the Biot number measures the heat transfer mechanism at the free surface, this means that the fluid system is more stable if the heat is allowed to escape from the fluid film to the surrounded air. In addition, when $B_i = 0$ the surface is thermally insulated and thus the free surface is the most unstable case since the whole transport of temperature in the system is still inside the fluid film.

The effects of shear-imposed stress on the critical Reynolds number for the Marangoni, Biot and elasticity numbers are established in the three parts of Fig. 7 respectively. The numerical calculations of the stability pictures that are shown in these parts, illustrated that all the three dimensionless numbers have the same influence on the stability behavior of the movement of the liquid film, which confirms the results obtained in Fig. 5 and 6. On the other hand, it is observed from Fig. 7 (c) that critical Reynolds number enlarged by the increasing of the elasticity number, while the opposite is true for increasing in the shear-imposed stress. This shows that the imposed shear stress plays a destabilizing role, while the surface surfactant has a stabilizing influence on the long-wave surface mode. In the absence of heat transfer, a similar result was reported by Bhat and Samanta (2019), in their study of the effect of shear-imposed on a contaminated falling film.

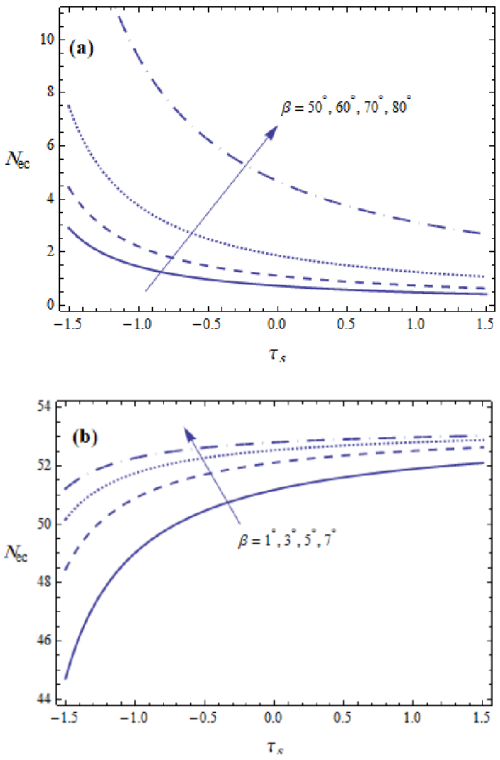


**Fig. 8. Neutral stability lines for long waves in the $N_{ec} - \tau_s$ plane, with $B_i = 0$ for the system parameters as considered in Fig. 6 Part (a) variation of large inclination angle $R_e = 0$. Part (b) variation of variation of small inclination angle $R_e = 5000$.**

Numerical computations at various of the inclination angle for zero and high Reynolds number are presented in the two parts of Fig. 8. The neutral stability curves for long wave approximation are illustrated in the plane $N_{ec} - \tau_s$. For larger angles, that drawn in Fig. 8(a) numerical estimations reveal that the neutral lines for the limiting case at $R_e = 0$ are increased due to an increase in small slope in the film plane. Also, it is observed from this graph that the critical elasticity number enhanced by the increase of

the slope angle, while the converse holds for growing the shear-imposed stress. This shows that there is a stabilization effect of the inclination angle and a destabilizing one on the regime. In Fig. 8(b) a small stepwise of increasing inclination angles at a high Reynolds number $R_e$ = 5000, the inspection of this shows that both of critical elasticity number and the shear-imposed stress extended due to enlarging in the slope angle, indicating the stable role of both, in which, the higher value of the Reynolds number has led to a shift in the role of shear stress from instability to stable. The considered numerical applications have shown that the film flow is sensitive to the substrate geometry (for example the angle of inclination), Marangoni parameter expressing the impact of thermal surface tension, Biot number, Reynolds number and surfactants through elasticity number.

## 4. CONCLUSIONS

In the present study, the free surface motion of a viscous liquid thin layer down an oblique heated plane is carried out. The free surface is subjected to additional fixed, shear stresses induced by an air-flow and insoluble surfactants are also presented on the air-liquid interface. The couple effects of temperature and surfactant concentration gradient on the surface tension are taken into account, in which the surface tension of the fluid is assumed to vary linearly on surfactant concentration and temperature. Depending on the linear stability problem, the exact analytical solutions for the Stokes flow ($R_e \rightarrow 0$) and the long-wave approximation ($k \rightarrow 0$) are derived. The stability conditions and the marginal lines are sketched and discussed. The underlying mechanisms of the stability behavior by the surfactant Péclet number, the Reynolds number, the Marangoni number, the surface tension through the capillary number, as well as the angle of inclination are considered and elucidated in detail.

Our results reveal that, the surfactant through the elasticity number and heat transfer mechanism at the free surface act as a stabilizer, while the Marangoni number has a destabilizing behavior on the movement of the fluid film. In the stabilization of long wave, the converse relation between the effect of Biot and Marangoni numbers is cleared. The angle of inclination and the surfactant Péclet number as well as the Reynolds number have destabilizing effects. The concentration of insoluble surfactant and the heat transfer process at the air-liquid interface have stabilizing impacts while the shear stress imposed by the air destabilizes the surface when it flows along the positive direction (down-hill). Finally, the results illustrated in this work can serve as a beneficial guide in developing the full stability configuration and it is interested in the oil burners, metal powder production, the spray coating process, and in microchips fabrication.

## REFERENCES

Alkharashi, S. A. (2019). A model of two viscoelastic liquid films traveling down in an inclined electrified channel, *Applied Mathematics and Computation* 355, 553-575.

Alkharashi, S. A., A. Assaf, K. Al-Hamad and A. Alrashidi, (2019). Performance Evaluation of In-soluble Surfactants on the Behavior of Two Electric Layers, *Journal of Applied Fluid Mechanics* 12(2), 573-586.

Barra, V., S. Afkhami, and L. Kondic, (2019). Thin viscoelastic dewetting films of Jeffreys type subjected to gravity and substrate interactions *The European Physical Journal E* 42(12), 1-14.

Bhat, F. A. and A. Samanta (2019). Linear stability analysis of a surfactant-laden shear-imposed falling film, *Physics Fluids* 31, 054103, 1-21.

Blyth, M. G. and C. Pozrikidis (2004). Effect of surfactant on the stability of film flow down an inclined plane, *Journal of Fluid Mechanics* 521, 241-250.

Ding, Z. and T. N. Wong (2013). Stability of a localized heated falling film with insoluble surfactants, *International Journal of Heat and Mass Transfer* 67, 627-636.

El-Sayed, M. F., N. T. Eldabe, M. H. Haroun and D. M. Mostafa (2013). Nonlinear electrohydrodynamic stability of two superposed Walters B' viscoelastic fluids in relative motionthrough porous medium, *Journal of Mechanics* 29, 569-582.

Frenkel, A. L. and D. Halpern (2002). Stokes-flow instability due to interfacial surfactant, *Physics Fluids* 14, L45-L48.

Gao, P. and X. Lu, (2007). Effect of surfactants on the inertialess instability of a two-layer film flow, *Journal of Fluid Mechanics* 591, 495-507.

Iqbal, M. R. S. (2013). Air-aided shear on a thin film subjected to a transverse magnetic field of constant strength: stability and dynamics, *ISRN Mathematical Physics*, 1-24.

Kwak, S. and C. Pozrikidis (2001). Effect of surfactants on the instability of a liquid thread or annular layer Part I: Quiescent fluids, *International Journal of Multiphase Flow* 27, 1-37.

Luo, H. and C. Pozrikidis (2007). Gravity-driven film flow down an inclined wall with three-dimensional corrugations, *Acta Mechanica* 188, 209-225.

Merkt, D., A. Pototsky and M. Bestehorn, (2005). Long-wave theory of bounded two-layer films with a free liquid-liquid interface: Short- and long-time evolution, *Physics Fluids* 17, 1-20.

Mikishev, A. B. and A. A. Nepomnyashchy (2010). Long-Wavelength Marangoni Convection in a Liquid Layer with Insoluble Surfactant: Linear Theory, *Microgravity Science and Technology* 22, 415-423.

Mukhopadhyay, A., and A. Mukhopadhyay (2009). Stability of conducting viscous film flowing

down an inclined plane with linear temperature variation in the presence of a uniform normal electric field, *International Journal of Heat and Mass Transfer* 52, 709-715.

Pop, I., and D. B. Ingham, (2001) *Convective Heat Transfer: Mathematical and Computational Modeling of Viscous Fluids and Porous Media*, Pergamon Press, Oxford.

Pozrikidis, C. (2003). Effect of surfactants on film flow down a periodic wall, *Journal of Fluid Mechanics* 496, 105-127.

Renardy, Y. and S. M. Sun (1994). Stability of a layer of viscous magnetic fluid flow down an inclined plane, *Physics Fluids* 6(10), 3235-3246.

Sadiq, I., R.Usha and S. W. Joo, (2010). Instabilities in a liquid film flow over an inclined heated porous substrate, *Chemical Engineering Science* 65, 4443-4459.

Samanta, A. (2008a). Stability of inertialess liquid film flowing down a heated inclined plane, *Physics Letters A* 372, 6653-6657.

Samanta, A. (2008b). Stability of liquid film falling down a vertical non-uniformly heated wall, *Physica D* 237, 2587-2598.

Samanta, A. (2014). Shear-imposed falling film, *Journal of Fluid Mechanics* 753, 131-149.

Shankar, V. (2005). Stability of two-layer viscoelastic plane Couette flow past a deformable solid layer: implications of fluid viscosity stratification, *Journal of Non-Newtonian Fluid Mechanics* 125, 143-158.

Smith, M. K. (1990). The mechanism for the long-wave instability in thin liquid films, *Journal of Fluid Mechanics* 217, 469-485.

Srivastava, A. and N. Tiwari (2018). Effect of an insoluble surfactant on the dynamics of a thin liquid film flowing over a non-uniformly heated substrate, *The European Physical Journal E* 41, 56.

Tomlin, R. J., S. N. Gomes, G. A. Pavliotis, and D. T. Papageorgiou (2019). Optimal Control of Thin Liquid Films and Transverse Mode Effects, *SIAM Journal on Applied Dynamical Systems* 18(1), 117-149.

Tseluiko, D. and D. T. Papageorgiou, (2006). Wave evolution on electrified falling films, *Journal of Fluid Mechanics* 556, 361-386.

Uma, B. and R. Usha (2006). Dynamics of a thin viscoelastic film on an inclined plane, *International Journal of Engineering Science* 44, 1449-1481.

Wei, H. (2004). Effect of surfactant on the long-wave instability of a shear-imposed liquid flow down an inclined plane, *Physics Fluids* 17, 1-5.

Yang, H., L. Jiang, K. Hu and J. Peng (2018) Numerical study of the surfactant-covered falling film flowing down a flexible wall, *European Journal of Mechanics / B Fluids* 72, 422-431.

Yih, C. S. (1963). Stability of liquid flow down an inclined plane, *Physics Fluids* 6, 321-334.

Zakaria, K. (2012). Long interfacial waves inside an inclined permeable channel, *International Journal of Non-Linear Mechanics* 47, 42-48.

Zijing, D., T. N. Wong (2013). Stability of a localized heated falling film with insoluble surfactants, *International Journal of Heat and Mass Transfer* 67, 627-636.